

# Palladium-Catalyzed Polymerization of Propene: DFT Model Studies

Artur Michalak<sup>†,‡</sup> and Tom Ziegler<sup>\*,†</sup>

Department of Chemistry, University of Calgary, University Drive 2500, Calgary, Alberta, Canada T2N 1N4, and Department of Theoretical Chemistry, Jagiellonian University, R. Ingardena 3, 30-060 Cracow, Poland

Received February 24, 1999

Gradient-corrected density functional theory has been used to study ethylene and propene polymerization catalyzed by  $N\wedge N$ -Pd<sup>II</sup> diimine complexes with  $N\wedge N = -NHCHCHNH-$  as a model ligand. Calculations have been carried out on the  $[N\wedge N-Pd^{II}R\{\eta^2-CH_2CHR'\}]^+$  polymerization precursor olefin complex (**1**; R' = H, CH<sub>3</sub>) as well as the alkyl insertion product  $[N\wedge N-Pd^{II}R']^+$  (**2**) with the alkyl chain R containing a primary, secondary, or tertiary  $\alpha$ -carbon. Both 1,2- and 2,1-insertions were considered for propene. The transition state TS (**1,2**) and the corresponding activation energies were determined for each investigated insertion process. Propene was found to prefer 2,1- over 1,2-insertion in all cases. The propene insertion barriers are higher than those of ethene and increase from **1** with R containing a primary  $\alpha$ -carbon to R containing a tertiary  $\alpha$ -carbon. Also considered was the isomerization process  $N\wedge N-Pd^{II}R''$  (**2**)  $\rightarrow$   $N\wedge N-Pd^{II}R'''$  (**2'**) by a  $\beta$ -hydrogen transfer process of the initial insertion product (**2**). A chain-straightening isomerization reaction following the 2,1-insertion toward alkyl groups (R''') with reduced substitution of the  $\alpha$ -carbon is not favorable. The relative stability of the isomers  $N\wedge N-Pd^{II}R'''$  (**2'**) follows the corresponding relative stability of the R''' radicals and would favor alkyl products with a high substitution on the  $\alpha$ -carbon. However, the final distribution of the  $N\wedge N-Pd^{II}R'''$  (**2'**) products is also determined by the polymerization precursor olefin complex  $[N\wedge N-Pd^{II}R\{\eta^2-CH_2CHR'\}]^+$  (**1**), for which steric factors favor low substitution at the  $\alpha$ -carbon.

## Introduction

The catalytic polymerization of olefins and copolymerization of olefins with monomers containing polar groups are of both technological and fundamental scientific interest. Recently, as an alternative to heterogeneous systems and group 4 metallocenes, a "second generation" of single-site olefin polymerization catalysts was introduced by Brookhart et al.<sup>1–4</sup> involving late-transition-metal complexes. The diimine Pd(II)- and Ni(II)-based catalysts made by Brookhart are not only able to polymerize  $\alpha$ -olefins<sup>1,2</sup> but also exhibit substantial tolerance toward polar functional groups on the monomer.<sup>3,4</sup> As in the case of metallocenes, by modification of the late-transition-metal-based catalyst structures one can potentially control the properties of the resulting polymers. Therefore, it is important to understand the factors that determine the relationship between catalyst structure and polymer properties. Here, the use of theoretical methods was shown to be very helpful for a number of transition-metal-based catalytic systems.<sup>5–28</sup>

Various aspects of ethene polymerization by Ni and Pd diimine complexes were the subject of recent theoretical studies.<sup>23–29</sup> Although some of the conclusions from these studies are transferable to other  $\alpha$ -olefins, new issues appear when the alkyl chain replaces an ethene hydrogen atom: e.g., the regioselectivity of the insertion. The chain-growing and isomerization reactions possible in the propene polymerization process are summarized in Scheme 1. The resting state of the catalyst is the olefin  $\pi$ -complex **1**.<sup>1</sup>

In general, two routes of olefin insertion are possible. The first involves the 1,2-insertion (reaction **1**) eventually leading to a  $\beta$ -agostic with a primary (unsubstituted) carbon atom of propene attached to the metal center. In the second, the 2,1-insertion (reaction **2**), the  $\beta$ -agostic complex **3** is formed, with a secondary (substituted) propene carbon linked to the Pd atom. It may be expected that in the presence of propene both

<sup>†</sup> University of Calgary.

<sup>‡</sup> Jagiellonian University.

(1) Johnson, L. K.; Killian, C. M.; Brookhart, M. *J. Am. Chem. Soc.* **1995**, *117*, 6414.

(2) Killian, C. M.; Tempel, D. J.; Johnson, L. K.; Brookhart, M. *J. Am. Chem. Soc.* **1996**, *118*, 11664.

(3) Johnson, L. K.; Mecking, S.; Brookhart, M. *J. Am. Chem. Soc.* **1996**, *118*, 267.

(4) Mecking, S.; Johnson, L. K.; Wang, L.; Brookhart, M. *J. Am. Chem. Soc.* **1998**, *120*, 888.

(5) Janiak, C. *J. Organomet. Chem.* **1993**, *452*, 63.

(6) Jolly, C. A.; Marynick, D. S. *J. Am. Chem. Soc.* **1989**, *111*, 7968.

(7) Castonguay, L. A.; Rappe, A. K. *J. Am. Chem. Soc.* **1992**, *114*, 5832.

(8) Proscenc, M.-H.; Brintzinger, H.-H. *Organometallics* **1997**, *16*, 3889.

(9) Kawamura-Kuribayashi, H.; Koga, N.; Morokuma, K. *J. Am. Chem. Soc.* **1992**, *114*, 2359.

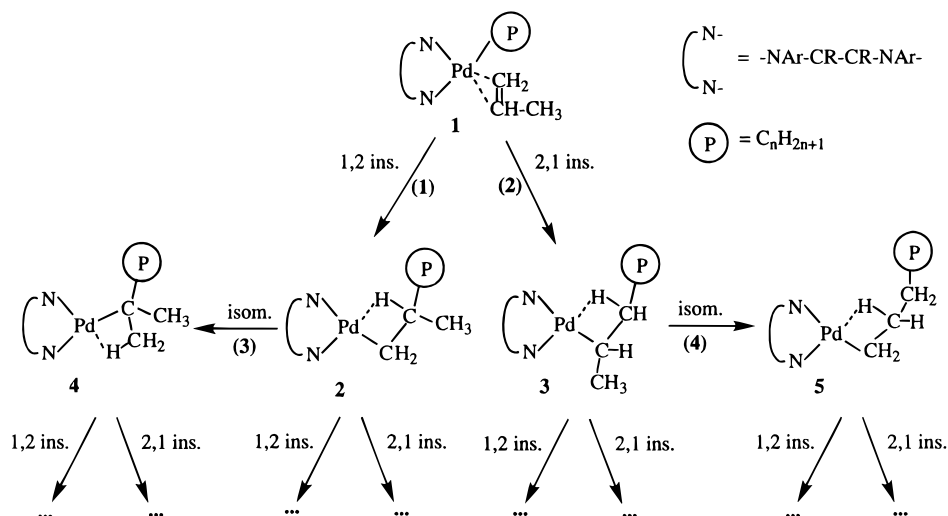
(10) Kawamura-Kuribayashi, H.; Koga, N.; Morokuma, K. *J. Am. Chem. Soc.* **1992**, *114*, 8687.

(11) Bierwagen, E. B.; Bercaw, J. E.; Goddard, W. A., III. *J. Am. Chem. Soc.* **1994**, *116*, 1481–1489.

(12) Gleiter, R.; Hyla-Kryspin, I.; Niu, S.; Erker, G. *Organometallics* **1993**, *12*, 3828.

(13) Mohr, R.; Berke, H.; Erker, G. *Helv. Chim. Acta* **1993**, *76*, 1389.

Scheme 1



insertion products will easily form new  $\pi$ -complexes from which new 1,2- or 2,1-insertions can proceed.

Alternatively, before the olefin uptake, the complexes **2** and **3** can isomerize. Thus, the complex **2** may rearrange to the complex **4**, with tertiary carbon atom connected to the metal atom (reaction **3**); yet another  $\beta$ -agostic complex **5**, with primary carbon forming the C–Pd bond, can be formed from the secondary complex **3** [reaction **4**]. Again, the polymer chain may grow further via the next 1,2- or 2,1-insertions, starting from the complexes **4** and **5**. Alternatively, they may rearrange to other  $\beta$ -agostics by further isomerizations. Thus, in the reactive system various species are present in which the metal atom forms bonds with primary, secondary, or tertiary carbon atoms.

After both, 1,2- and 2,1-insertions one methyl branch is introduced. If no isomerization took place, the resulting polymer chain would have a regular number of 333.33 methyl branches per 1000 carbon atoms in the case of propene, and  $1000/n$  branches per 1000 carbons in the case of higher  $\alpha$ -olefins comprising  $n$  carbon atoms. The isomerization reaction (reaction **3**) introduces an additional methyl branch, while reaction **4**

leads to straightening of the chain, since it removes a methyl branch. It has been observed experimentally<sup>1,2</sup> that in  $\alpha$ -olefin polymerization reactions catalyzed by diimine Pd and Ni complexes the resulting number of branches is substantially lower than that expected from regular, subsequent insertions, e.g. 150–300 for polypropene and 70–160 for polyhexene. An explanation of these experimental observations assumes that the ratio of 1,2- to 2,1-insertion is the main factor controlling the degree of branching, i.e., that the 1,2-insertions occur more often, and all the 2,1-insertions are immediately followed by chain-straightening reactions.<sup>1,2</sup>

The main purpose of the present investigation is to conduct a computational study of the relative stability of the different species present in the catalytic cycle as well as the activation barriers of the elementary steps in the Pd-catalyzed propene polymerization process. Our calculations will be based on density functional theory (DFT), and the N $\wedge$ N diimine ligands employed by Brookhart will be modeled by N $\wedge$ N = –NHCHCHNH–. Activation barriers are reported for the 1,2- and 2,1-propene insertion reactions into the Pd–C bonds with primary, secondary, and tertiary  $\alpha$ -carbons. The results obtained for propene insertion are compared with the corresponding data for ethene insertion. In addition, a discussion will be presented of the activation barriers for the isomerization reactions in Scheme 1. Finally, we will discuss the relative stabilities of the different alkyl and olefin groups involving propyl and butyl isomers.

### Computational Details and the Model Systems

All the results were obtained from DFT calculations using the Amsterdam Density Functional (ADF) program.<sup>30–35</sup> Double- $\zeta$  STO basis sets with polarization functions were applied for H, C, and N atoms, while a triple- $\zeta$  basis set was employed

(14) Froese, R. D. J.; Musaev, D. G.; Matsubara, T.; Morokuma, K. *J. Am. Chem. Soc.* **1997**, *119*, 7190.

(15) Weiss, H.; Ehrig, C.; Ahlrichs, R. *J. Am. Chem. Soc.* **1994**, *116*, 4919.

(16) Yoshida, T.; Koga, N.; Morokuma, K. *Organometallics* **1995**, *14*, 746.

(17) Margl, P.; Deng, L.; Ziegler, T. *J. Am. Chem. Soc.* **1998**, *120*, 5517–5525.

(18) Margl, P.; Deng, L.; Ziegler, T. *Organometallics* **1998**, *17*, 933.

(19) Woo, T. K.; Margl, P.; Ziegler, T.; Blöchl, P. E. *Organometallics* **1997**, *16*, 3454.

(20) Woo, T.; Margl, P. M.; Lohrenz, J. C. W.; Blöchl, P. E.; Ziegler, T. *J. Am. Chem. Soc.* **1996**, *118*, 13021.

(21) Woo, T. K.; Fan, L.; Ziegler, T. *Organometallics* **1994**, *13*, 432.

(22) Woo, T. K.; Fan, L.; Ziegler, T. *Organometallics* **1994**, *13*, 2252.

(23) Margl, P.; Deng, L.; Ziegler, T. *J. Am. Chem. Soc.* **1999**, *121*, 154.

(24) Deng, L.; Margl, P.; Ziegler, T. *J. Am. Chem. Soc.* **1997**, *119*, 1094.

(25) Deng, L.; Woo, T. K.; Cavallo, L.; Margl, P. M.; Ziegler, T. *J. Am. Chem. Soc.* **1997**, *119*, 6177.

(26) Musaev, D. G.; Svensson, M.; Morokuma, K.; Strömberg, S.; Zetterberg, K.; Siegbahn, P. E. M. *Organometallics* **1997**, *16*, 1933.

(27) Froese, R. D. J.; Musaev, D. G.; Morokuma, K. *J. Am. Chem. Soc.* **1998**, *120*, 1581.

(28) Musaev, D. G.; Froese, R. D. J.; Morokuma, K. *Organometallics* **1998**, *17*, 1850.

(29) Deng, L.; Margl, P.; Ziegler, T. Manuscript in preparation.

(30) Baerends, E. J. Ph.D. Thesis, Free University, Amsterdam, The Netherlands, 1973.

(31) Baerends, E. J.; Ellis, D. E.; Ros, P. *Chem. Phys.* **1973**, *2*, 41.

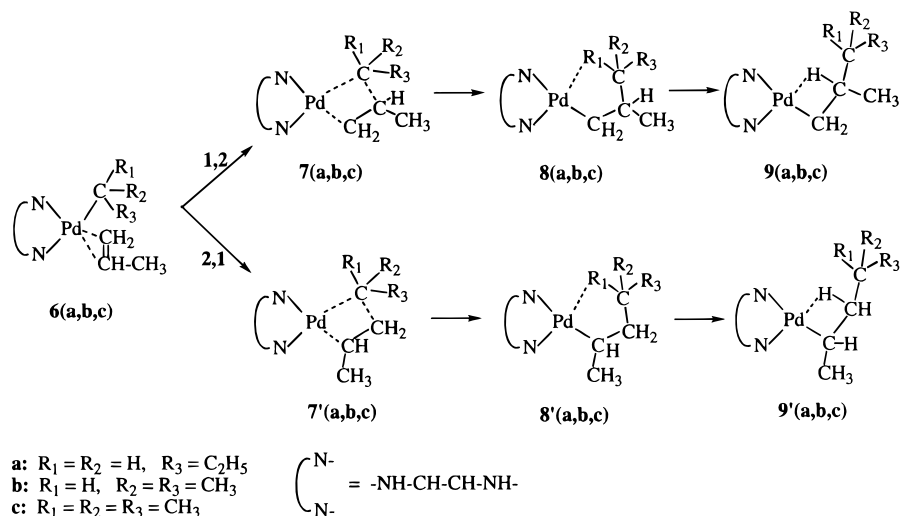
(32) Ravenek, W. In *Algorithms and Applications on Vector and Parallel Computers*; te Riele, H. J. J., Dekker, T. J., van de Horst, H. A., Eds.; Elsevier: Amsterdam, The Netherlands, 1987.

(33) te Velde, G.; Baerends, E. J. *J. Comput. Chem.* **1992**, *99*, 84.

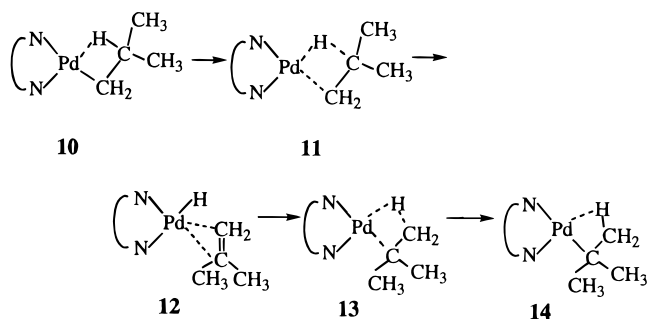
(34) Boerrigter, P. M.; te Velde, G.; Baerends, E. J. *Int. J. Quantum Chem.* **1988**, *33*, 87.

(35) Versluis, L.; Ziegler, T. *J. Chem. Phys.* **1988**, *88*, 322.

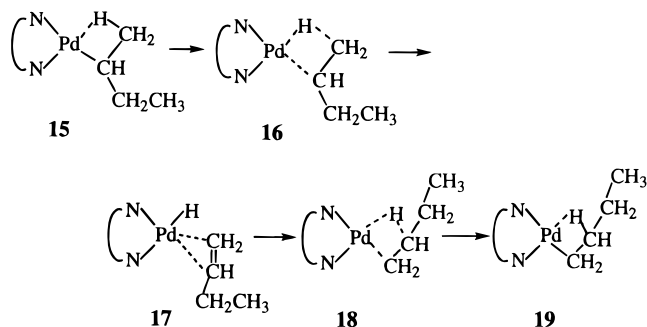
Scheme 2



Scheme 3



Scheme 4



for the Pd atom.<sup>36,37</sup> The 1s electrons of C and N and the 1s–3d electrons of Pd were treated as a frozen core. The auxiliary<sup>38</sup> s, p, d, f, and g STO functions, centered on all nuclei, were used to fit the electron density and the Coulomb and exchange potentials in each SCF cycle. The Becke–Perdew exchange–correlation functional was used in all the calculations.<sup>39–41</sup> The reported energy differences include first-order scalar relativistic correction,<sup>42–44</sup> since it has been shown<sup>45</sup> that such an approach is sufficient for 4d transition-metal atoms.

The Pd-based diimine catalyst was modeled by a  $\text{N}\wedge\text{N}-\text{Pd}^+$  complex, with  $\text{N}\wedge\text{N} = -\text{NHCHCHNH}-$ . In the studies of the 1,2- and 2,1-insertion reactions into the Pd–C bond involving primary, secondary, and tertiary  $\alpha$ -carbons, the *n*-propyl, isopropyl, and *tert*-butyl groups were used to model the alkyl chain, respectively. The systems studied are shown in Scheme 2; DFT calculations have been performed for the corresponding  $\pi$ -complexes (**6a–c**), insertion transition states (**7a–c**, **7'a–c**), the  $\gamma$ -agostic complexes (**8a–c**, **8'a–c**), and the  $\beta$ -agostic (**9a–c**, **9'a–c**) alkyl complexes. The complex **6a** with a primary

$\alpha$ -carbon attached to the Pd atom may serve as a general model for the  $\pi$ -complexes formed from the species **2** and **5** of Scheme 1, since in both of them a primary carbon is linked to Pd; complexes **6b** and **6c**, with secondary and tertiary  $\alpha$ -carbons linked to the metal, represent models for the corresponding complexes formed from **3** and **4**, respectively.

For the  $\beta$ -agostic alkyl complexes **2** and **4**, the reactant and product in the isomerization reaction (**3**) of Scheme 1 were modeled by the corresponding complexes **10** and **14** (see Scheme 3) with isobutyl and *tert*-butyl groups replacing the alkyl chain, respectively. The mechanism of this reaction involves hydrogen abstraction, which leads to the olefin–hydride complex **12** via the transition state **11** followed by rotation of olefin and reinsertion of hydrogen via the transition state **13**.

Similarly for the  $\beta$ -agostic complexes, the olefin–hydride complex and the transition states in the chain-straightening reaction (**4**) of Scheme 1 are shown in Scheme 4 (**15–19**). Here the *sec*- and *n*-butyl groups were used to model the  $\beta$ -agostic compounds **3** and **5**, respectively. A previous computational study of reaction **3** reported three different metal hydride olefin complexes with similar energies.<sup>28</sup> However, it is not clear, whether they constitute stable minima on the potential energy surface or represent transition states.<sup>29</sup> Since this problem is not crucial for our considerations, we present only the highest energy transition states for both isomerization reaction.

Finally, calculations were also performed for all the propene  $\pi$ -complexes involving different butyl groups modeling the alkyl chain, to facilitate the comparison of their relative stabilities.

## Results and Discussion

Relative energies for the stationary points of the 1,2- and 2,1-propene insertion reactions given in Scheme 2

(36) Snijders, J. G.; Baerends, E. J.; Vernoijs, P. *At. Nucl. Data Tables* **1982**, *26*, 483.

(37) Vernoijs, P.; Snijders, J. G.; Baerends, E. J. Slater Type Basis Functions for the Whole Periodic System, Internal report (in Dutch); Department of Theoretical Chemistry, Free University, Amsterdam, The Netherlands, 1981.

(38) Krijn, J.; Baerends, E. J. Fit Functions in the HFS Method, Internal Report (in Dutch); Department of Theoretical Chemistry, Free University, Amsterdam, The Netherlands, 1984.

(39) Becke, A. *Phys. Rev. A* **1988**, *38*, 3098.

(40) Perdew, J. P. *Phys. Rev. B* **1986**, *34*, 7406.

(41) Perdew, J. P. *Phys. Rev. B* **1986**, *33*, 8822.

(42) Ziegler, T.; Tschinke, V.; Baerends, E. J.; Snijders, J. G.; Ravenek, W. *J. Phys. Chem.* **1989**, *93*, 3050.

(43) Snijders, J. G.; Baerends, E. J. *Mol. Phys.* **1978**, *36*, 1789.

(44) Snijders, J. G.; Baerends, E. J.; Ros, P. *Mol. Phys.* **1979**, *38*, 1909.

(45) Deng, L.; Ziegler, T.; Woo, T. K.; Margl, P.; Fan, T. *Organometallics* **1998**, *17*, 3240.

**Table 1. Relative Energies<sup>a</sup> for the Stationary Points in the 1,2- and 2,1-Propene Insertion Reactions into the Pd–Alkyl Bond Involving the Primary, Secondary, and Tertiary Carbon Atoms (See Scheme 2)**

structure	relative energy <sup>a</sup> (kcal/mol)					
	primary		secondary		tertiary	
$\pi$ -complexes	<b>6a</b>	–20.85 (0.00)	<b>6b</b>	–20.08 (0.00)	<b>6c</b>	–14.13 (0.00)
TS	1,2	<b>7a</b> +1.87 (+22.72)	<b>7b</b>	+5.94 (+26.02)	<b>7c</b>	+15.18 (+29.31)
	2,1	<b>7'a</b> –0.18 (+20.67)	<b>7'b</b>	+1.87 (+21.95)	<b>7'c</b>	+11.52 (+25.65)
$\gamma(\delta)$ -agostic <sup>b</sup>	1,2	<b>8a</b> –15.64 (+5.21)	<b>8b</b>	–13.23 (+6.85)	<b>8c</b>	–15.68 (–1.55)
	2,1	<b>8'a</b> –16.80 (–4.05)	<b>8'b</b>	–15.71 (+4.37)	<b>8'c</b>	–17.10 (–2.97)
$\beta$ -agostic	1,2	<b>9a</b> –23.02 (–2.17)	<b>9b</b>	–21.71 (–1.63)	<b>9c</b>	–17.59 (–3.46)
	2,1	<b>9'a</b> –24.91 (–4.06)	<b>9'b</b>	–24.26 (–4.18)	<b>9'c</b>	–21.31 (–7.18)

<sup>a</sup> With respect to the isolated reactants (propene + corresponding  $\beta$ -agostic alkyl complex), and to the  $\pi$ -complexes (in parentheses). <sup>b</sup>  $\delta$ -agostic, due to the lack of  $\gamma$ -hydrogens, in the case of **8c** and **8'c**.

**Table 2. Relative Energies<sup>a</sup> for the Stationary Points in the Ethylene Insertion Reactions into the Pd–Alkyl Bond Involving the Primary, Secondary, and Tertiary Carbon Atoms**

structure	relative energy <sup>a</sup> (kcal/mol)		
	primary	secondary	tertiary
$\pi$ -complexes	–18.82 (0.00)	–18.18 (0.00)	–12.45 (0.00)
TS	+0.01 (+18.83)	+1.97 (+20.15)	+11.33 (+23.78)
$\gamma(\delta)$ -agostic <sup>b</sup>	–16.92 (+1.90)	–15.47 (+2.71)	–18.62 (–6.17)
$\beta$ -agostic	–24.47 (–5.65)	–23.24 (–5.06)	–20.87 (–8.42)

<sup>a</sup> With respect to the isolated reactants (ethylene + corresponding  $\beta$ -agostic alkyl complex) and to the  $\pi$ -complexes (in parentheses). <sup>b</sup>  $\delta$ -agostic, due to the lack of  $\gamma$ -hydrogens, in the case of the tertiary system.

**Table 3. Relative Energies<sup>a</sup> for the Stationary Points in the Isomerization Reactions (see Schemes 3 and 4)**

reaction	relative energy <sup>a</sup> (kcal/mol)		
	$\beta$ -agostic	TS <sup>b</sup>	$\beta$ -agostic
(3)	<b>10</b> 0.00	<b>13</b> +4.56	<b>14</b> –3.42
(4)	<b>15</b> 0.00	<b>16</b> +5.84	<b>19</b> +1.59

<sup>a</sup> With respect to corresponding  $\beta$ -agostic insertion products. <sup>b</sup> The highest energy TS along the preferred reaction path (see text).

are listed in Table 1. For comparison, results from ethene insertion are summarized in Table 2. Relative energies of stationary points related to the isomerization reactions are recorded in Table 3, while the relative energies of the butyl complexes are analyzed in Table 4. Finally, Table 5 compares the relative stabilities of alkyl and propene  $\pi$ -complexes, involving different propyl and butyl groups.

**A. Olefin  $\pi$ -Complexes.** Propene can adopt a number of different conformations as it coordinates to an alkyl complex. Figure 1 displays four “perpendicular” conformations involving different orientations of the propene methyl group as propene coordinates to a *n*-propyl complex with the double bond perpendicular to the diimine coordination plane. It comes as no surprise that the most stable conformation (**6a**) has the methyl group on the opposite side of both the ring and the C=C bond, relative to the alkyl chain. The energetic order of these four complexes clearly follows the repulsion between the methyl and alkyl groups: the more distant these groups are, the lower the energy. In addition to these four “perpendicular” conformations, one could also envision four “parallel” structures with the double C=C bond in the diimine coordination plane. However, in the case of these “parallel” propene complexes the local minima either do not exist at all or are

**Table 4. Fragment Analysis of Differences in the Total Energies of the Alternative  $\beta$ -Agostic Complexes (10 and 14, 15 and 19; See Schemes 3 and 4)**

Systems		
A	$N\Delta N-Pd^{+}$	$N\Delta N-Pd^{+}$
B	$\bullet CH_2CH(CH_3)_2$	$\bullet CH(CH_3)C_2H_5$
C	$\bullet C(CH_3)_3$	$\bullet CH_2CH_2CH_2CH_3$
A–B	<b>10</b>	<b>15</b>
A–C	<b>14</b>	<b>19</b>
Energy Differences		
$E_1 = E(A-C) - E(A-B)$	–3.42	+1.59
$E_2 = E(C) - E(B)^a$	–5.49	+2.89
$E_3 = E(C) - E(B)^b$	–9.03	+4.57
$E_4 = E(A-B) - E(A) - E(B)^b$	–81.78	–77.89
$E_5 = E(A-C) - E(A) - E(C)^b$	–76.73	–80.47
$E_6 = E_5 - E_4$	+5.05	–2.58
$E_7 = E_1 - E_3 - E_6$	+0.56	–0.40

<sup>a</sup> Isolated fragment geometries. <sup>b</sup> Distorted fragment geometries (as in the A–B or A–C systems).

**Table 5. Relative Energies<sup>a</sup> for the  $\beta$ -Agostic and Propene  $\pi$ -Complexes Comprising Propyl and Butyl Groups Compared with the Corresponding Energy Differences for Alkyl Radicals**

alkyl	relative energy <sup>a</sup> (kcal/mol)		
	$\beta$ -agostic complex	$\pi$ -complex $N\Delta N-Pd-(alkyl)-$ (propene)	alkyl radicals
<i>n</i> -propyl	1.96	1.20	6.32
isopropyl	0.00	0.00	0.00
<i>n</i> -butyl	4.95	0.53	6.72
isobutyl	3.42	1.01	5.48
<i>sec</i> -butyl	2.12, 3.36 <sup>b</sup>	0.00	3.83
<i>tert</i> -butyl	0.00	1.82	0.00

<sup>a</sup> With respect to the most stable corresponding complex/radical. <sup>b</sup> With Pd–H agostic bonds involving ethyl and methyl hydrogens, respectively.

so shallow that the geometry optimizations eventually lead to the “perpendicular” complexes. Preference for the perpendicular coordination of olefins is a result of a lower steric repulsion between the olefin molecule and the alkyl chain. The corresponding “parallel” ethylene complex forms a stable minimum that is higher in energy by 5.25 kcal/mol compared to “perpendicular” conformation.

It is seen from Figure 1 that the Pd–C bonds involving the unsubstituted carbon in the propene  $\pi$ -complexes are shorter by 0.06–0.09 Å. The same is true for propene  $\pi$ -complexes with secondary and tertiary  $\alpha$ -carbons on the alkyl chain attached to Pd. In these systems the Pd–C(olefin) bonds do not change much in comparison to the “primary” systems of Figure 1. However, the Pd–C(alkyl) bond becomes longer (2.07,

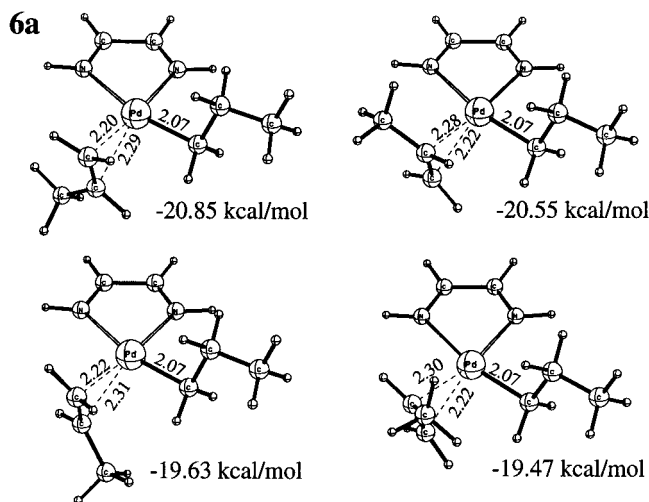


**Figure 1.** Geometries of four alternative propene  $\pi$ -complexes, together with their stabilization energies (kcal/mol) and the Pd–C bond lengths (Å).

2.09, and 2.13 Å for the primary, secondary, and tertiary carbons, respectively). The shorter Pd–C bond distance involving the unsubstituted carbon atom in propene complexes can readily be explained by a polarization of the  $\pi$ -orbital in propene toward the  $\text{CH}_2$  group.

A comparison of the  $\pi$ -complex stabilization energies (first row of Table 1) shows that in all cases the olefin uptake is strongly exothermic. However, the stabilization energies of the secondary and tertiary systems in comparison to the primary one are decreased by 0.77 and 6.72 kcal/mol, respectively. The dramatic effect observed in the tertiary system is a result of both decreased stability of the  $\pi$ -complex itself, and increased stability of the mother alkyl  $\beta$ -agostic complex. This aspect will be discussed later in more detail (see Table 5).

From a comparison of Tables 1 and 2 it is seen that the propene stabilization energy is always larger than that of ethene, by 2.03, 1.90, and 1.68 kcal/mol for the primary, secondary, and tertiary systems, respectively. An increased stability of propene  $\pi$ -complexes results from destabilization of its HOMO orbital in comparison to ethene, which facilitates the propene  $\rightarrow$  Pd charge transfer. From our calculations the HOMO  $\pi$ -orbital energies for propene and ethene are  $-6.65$  and  $-7.16$  eV, respectively. The trend in  $\pi$ -complexation energies is in contradiction with experimental results,<sup>4</sup> showing that ethene binds more strongly than  $\alpha$ -olefins. One should remember, however, that the present results were obtained for the model catalyst, without large substituted aryl groups on the diimine ligands. That is, in the real systems the electronic factor is overridden by steric factors which favor the smaller ethene ligand.

**B. 1,2- vs 2,1-Insertion of Propene.** Starting from the four perpendicular propene conformations of Figure 1, four insertion paths can be envisioned as propene is brought into the diimine coordination plane. However, the first and last conformation will produce the same in-plane conformations, and this is also true for the remaining two perpendicular propene complexes. There-

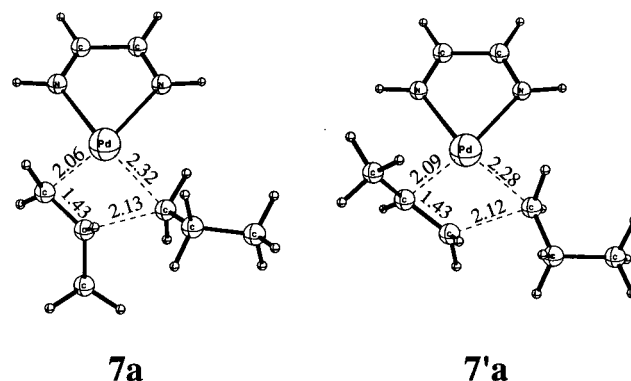


**Figure 2.** Geometries of transition states for the 1,2- and 2,1-propene insertion into the Pd–C bond with primary carbon atoms, together with the crucial bond lengths (Å).

fore, only two 1,2- and two 2,1-insertion paths exist. The results presented in Table 1 correspond to the energetically preferred 1,2- and 2,1-paths, with the most stable olefin complexes used as the reference points.

To illustrate this point, the two 1,2- and 2,1-insertion transition state structures, for the *n*-propyl system, are shown in Figure 2. As in the case of ethene, the four atoms forming new bonds are roughly planar; the same is true for the remaining TS involving secondary and tertiary carbon atom.

The results listed in Table 1 clearly show that in all the cases 2,1-insertion is strongly preferred. That is, the 2,1-insertion barriers are lower, in comparison to those of 1,2-insertion, by 2.05, 4.06, and 3.66 kcal/mol for the primary, secondary, and tertiary systems, respectively. The preference of 2,1-insertion for propene comes mainly from the fact that in all the transition states the bonds around the propene carbon atom that forms the C–C bond to the  $\alpha$ -carbon of the alkyl chain are bent more by angular distortions in the transition state than those around the  $\alpha$ -carbon itself. Since the angular distortion of a C–H bond (only distortion possible in 2,1-insertion) costs less energy than an angular distortion of a C–C bond (possible in 1,2-insertion), the distortion energy of propene in the 2,1-insertion TS is lower than in the 1,2-insertion TS by 1.70 kcal/mol, for the primary system. The total distortion energies of the two propenes are 17.46 and 15.76 kcal/mol for 1,2- and 2,1-insertion TS, respectively. It should also be noticed that these values represent ca. 76% of the corresponding activation energies. The calculated preference for the 2,1-propene insertion is in agreement with experimental results.<sup>1</sup>

A comparison of the propene and ethene insertion barriers shows that insertion of ethene is always more favorable than the 2,1-propene insertion by 1.8–1.9 kcal/mol. This originates again from the difference in ethene and propene distortion energies, which is 1.71 kcal/mol for the geometries of the corresponding “primary” transition states. This is again in agreement with experimental data for the real catalysts, showing lower insertion rates for propene.<sup>1</sup>

An inspection of the results of Table 1 shows that not only are the 2,1-insertion barriers lower than those from 1,2-insertion but also the stabilization of the 2,1-reaction products is larger. In all the cases both the kinetic,  $\gamma$ -agostic, and thermodynamic,  $\beta$ -agostic, 2,1-insertion products have lower energy than those corresponding to the 1,2-insertion.

**C. Chain Isomerization Reactions and Relative Stability of Isomers.** The results of Table 3 indicate that the activation energies for isomerization of the 1,2- and 2,1-insertion products are much lower than the insertion barriers. However, while the isomerization reaction (3), which occurs after 1,2-insertion, leads to the more stable  $\beta$ -agostic product 14, the chain-straightening reaction (4), following the preferred 2,1-insertion, leads to the complex 19, which is less stable by 1.59 kcal/mol than the insertion product 15.

To explain the relative stability of the alternative  $\beta$ -agostic products, fragment analysis of these systems was performed, and the results are presented in Table 4. It seems to be the stability of the corresponding alkyl radical that is the main factor responsible for the preference of a given isomer. Indeed, in the case of reaction (3), the *tert*-butyl radical is more stable by 5.49 kcal/mol than the isobutyl radical. This difference increases to 9.03 kcal/mol, when the distortion energies, corresponding to the complex geometries, are taken into account. On the other hand, the bonding energy of the *tert*-butyl group is lower than that of the isobutyl radical by 5.05 kcal/mol. It should be noticed at this point that the energies  $E_4$  and  $E_5$  include the effects of both Pd–C bond formation and the Pd–H agostic interaction. Weakening of these two bonds is also reflected by their lengths, increasing from 2.07 and 1.77 Å in the *tert*-butyl complex, to 2.10 and 1.85 Å in the isobutyl system. Similarly, in the case of reaction 4 the *sec*-butyl radical is more stable than the *n*-butyl radical by 2.98 and 4.57 kcal/mol, for the minimum energy and distorted geometries, respectively, and its bonding energy is lower by 2.58 kcal/mol. The energy differences  $E_7$  presented in the last row of Table 4 indicate that the change in geometry of the N $\wedge$ N–Pd<sup>+</sup> fragment in a given two  $\beta$ -agostic complexes has only a minor influence on their relative stability.

Table 5 lists the relative energies of the  $\beta$ -agostic alkyl complexes and the propene  $\pi$ -complexes involving all different propyl and butyl isomers. Also shown are the corresponding relative energies of the alkyl radicals. A comparison of the first and third columns of the table shows that indeed the energetic order of  $\beta$ -agostic alkyl complexes reflects that of the corresponding radicals. However, the energy differences between  $\beta$ -agostic isomers are decreased, in comparison to those of the radicals, since the bond involving the more stable alkyl is weaker than that involving the less stable alkyl radical. A comparison of the second and third column indicates that in the case of propene  $\pi$ -complexes the order of isomers is different. Here, the most stable isomer is the complex containing the *sec*-butyl group, followed by those with *n*-butyl and isobutyl. The *tert*-butyl  $\pi$ -complex has the highest energy. It may be concluded that in the  $\pi$ -complexes the steric overcrowding together with the previously mentioned Pd–C bond weakening dominate over the stability of the corresponding radicals, thus changing the energetic hierarchy of the isomer complexes.

A comparison between the results of Table 5 for propyl and butyl complexes shows that in the latter case the difference between energies of complexes with Pd–C bonds involving primary and secondary carbons is decreased from 1.96 to 1.59 kcal/mol for the  $\beta$ -agostic alkyl

systems and from 1.20 to 0.53 kcal/mol for propene  $\pi$ -complexes. This a posteriori justifies the use of propyl systems in modeling of the propene insertion into the Pd–C bond with primary and secondary carbons, since both the  $\beta$ -agostic and  $\pi$ -complex energy differences are decreased by approximately the same amount. Thus, the relative energies presented in Table 1 would not change much if butyl groups were used instead of propyl chains.

**D. Implications for Polymer Branching.** As has already been mentioned in the Introduction, either 1,2- or 2,1-insertions would lead to a regular number of 333 branches per 1000 C. The experimentally observed<sup>1,2</sup> lower degree of polyolefin branching could be explained by a chain straightening reaction (reaction 4) following the 2,1-insertion. Therefore, the ratio of 2,1- to 1,2-insertion was assumed in a discussion of experimental findings to be the factor controlling branching in these systems.<sup>1,2,4</sup> However, the results presented in the preceding sections indicate that it is not only the ratio between the two insertions that is important here. The 2,1-insertion into the Pd–C bond with primary carbon is strongly favorable, and the energy difference between the 2,1- and 1,2-insertion barriers is increased in the case of secondary and tertiary systems. It should be noticed that the difference of 2.05 kcal/mol in the primary system corresponds to a ratio in the frequency of 2,1- over 1,2-insertion of 1:30 at 300 K. Thus, if the chain straightening reaction (4) was always following the 2,1-insertion, it would lead to almost linear polyolefin.

The results presented in section C show that the chain-straightening reaction is not thermodynamically favorable, however. The energy difference between the alternative  $\beta$ -agostic complexes, modeled with *sec*- and *n*-butyl groups, has been found to be 1.59 kcal/mol. This relatively high energy difference would mean that only every 14th 2,1-insertion would be followed by isomerization reaction 4 at 300 K; this corresponds to a slightly decreased number of 311 branches per 1000 C in polypropene, still higher than experimentally observed results. However, since the resting state of the catalyst is an olefin  $\pi$ -complex,<sup>1</sup> the equilibrium between the alternative  $\pi$ -complexes with primary and secondary alkyl groups must be taken into account as well. From our results, the difference in energies of the two complexes is 0.53 kcal/mol only, which corresponds to a ratio of 2:5 at 300 K, with the preference for the secondary system. If this were the only factor controlling the polymer branching, it would give 237 branches per 1000 C. This value is in the middle of the experimentally observed range for real Pd- and Ni-containing catalysts (150–300).<sup>1,2</sup>

Therefore, from the present results, it seems that it is the equilibrium between the alternative  $\pi$ -complexes that is the main factor controlling polymer branching. One should remember, however, that the present results were obtained for the model system. Including the aryl groups with bulky ortho substituents, present in real catalysts, will affect all three factors, i.e., the ratio of 1,2- to 2,1-insertion as well as the equilibria between alternative  $\beta$ -agostic and  $\pi$ -complexes; therefore, all of them should be taken into account in discussing the branching of real systems.

### Concluding Remarks

We have reported results of the DFT investigations of propene polymerization catalyzed by Pd(II)-diimine complexes, modeled with  $N\wedge N = -NHCHCHNH-$ . The two alternative propene insertions into the Pd-C bond with primary, secondary, and tertiary carbons and the subsequent isomerization reactions have been studied and compared with the corresponding results for ethene.

The propene  $\pi$ -complexes with the model catalyst are stabilized more strongly than the corresponding ethene complexes, while the reverse trend has been observed experimentally, as a result of steric factors in real catalytic systems. An asymmetry in the two Pd-C bonds in propene  $\pi$ -complexes was found, resulting from the asymmetry in propene frontier orbitals. For the systems with primary, secondary, and tertiary alkyl carbons attached to the metal, the  $\pi$ -complex stabilization energies decrease, while the insertion barriers increase.

The 2,1-regioselectivity of propene insertion is strongly preferred for all the model systems: the activation energies of 2,1- and 1,2-insertions differ by 2.05, 4.06, and 3.66 kcal/mol for the systems with primary, secondary, and tertiary carbon atoms attached to the metal, respectively. In agreement with experimental results, the propene insertion barriers have been found to be higher than that of ethene.

The chain-straightening isomerization reaction, following the 2,1-insertion, is not favorable: neither the  $\beta$ -agostic nor the propene  $\pi$ -complexes with primary

alkyl chains are preferred. The relative stability of alternative isomers follows that of alkyl radicals in the case of  $\beta$ -agostic alkyl complexes: the tertiary complex is the most stable, and the primary complex has the highest energy. This energetic hierarchy of the isomers changes in the case of propene  $\pi$ -complexes: as a result of steric demand and Pd-C bond weakening the complex with a *tert*-butyl group becomes the least stable; the system with a *sec*-butyl group is preferred, followed by those with *n*-butyl and isobutyl groups.

Our results suggest that it is not only the ratio of 2,1- to 1,2-insertions that controls the extent of branching in polyolefin systems; relative stabilities of the alternative  $\beta$ -agostic and  $\pi$ -complexes are even more important for a model catalyst and, therefore, should be considered for real systems as well.

**Acknowledgment.** This work has been supported by the National Sciences and Engineering Research Council of Canada (NSERC), as well as by the donors of the Petroleum Research Fund, administered by the American Chemical Society (ACS-PRF No. 31205-AC3).

**Supporting Information Available:** Optimized geometries of the crucial structures reported (Cartesian coordinates, in Å). This material is available free of charge via the Internet at <http://pubs.acs.org>.

OM990134P